C98-07-12
contribution
edited by A. Ohsawa
10
ICRR-REPORT-434-98-30A
October 1998
FERMILAB
DEC 14 1998
LIBRARY
ICRR-434-98-30A
Fermilab Library
0 1160 0056140 3

Emulsion Chamber Experiment at Mt. Chacaltaya
— *Multiple Particle Production and Centauro Events* —

A.Ohsawa [a] and Chacaltaya Emulsion Chamber Collaboration

[a] *Institute for Cosmic Ray Research, University of Tokyo, Tanashi, Tokyo.*

A review is made on the features of multiple particle production and the Centauro events, based on the data which are obtained by Chacaltaya emulsion chamber experiment. Discussion follows on the point whether the Feynman scaling law is holding or violated in 10^{14}, 10^{16} and 10^{18} eV, and on the origin of Centauro events.

1. Features of Multiple Particle Production in 10^{14} eV

Emulsion Chamber Experiment has been carried out at Mt. Chacaltaya (5,200 m, Bolivia), aiming mainly at studying nuclear interactions in the energy region exceeding those of the accelerators.[1, 2]

Emulsion chamber, a multiple sandwich of lead plates and sensitive layers (X-ray films and/or a nuclear emulsion plate), is a detector of electron showers which are produced in the chamber through the cascade process by the incident electron (or photon). It has the space and energy resolutions of $\Delta x = 10 \sim 50$ μm and $\Delta E/E = 10 \sim 20$ %, respectively, and the detection threshold $E_{th} \sim 1$ TeV. A hadron is also detected (called "Pb-jets") because it produces a bundle of γ-rays through a nuclear collision with Pb. However, hadron detection is limited, because the collision mean free path of hadrons is long (18.5 cm) in the chamber and because the γ-rays to produce a shower carry only a part of the hadron energy, *i.e.* $E_h^{(\gamma)} = k_\gamma E_h$.

Two-storied emulsion chamber (44.2 m^2), which showed the best performance, consists of the upper chamber (6 cm Pb), the target layer (30 cm $(CH_2)_n$), the air gap (237 cm) and the lower chamber (10 cm Pb). (Fig. 1) The hadrons, incident upon the chamber, causes a nuclear collision in the target layer (called 'C-jet') and the produced γ-rays are detected by the lower chamber, having mutual distances enough to be identified individually through the divergence in the air gap. It is an advantage of C-jets that the energies of γ-rays can be calibrated by the kinematical relation of $\pi^0 \to 2\gamma$ decay. That is, the errors of the interaction height (assuming that the interaction point is at the center of the target layer) and the relative distance of γ-rays are $\Delta H/H < 0.06$ and $\Delta x/x < 0.05$, respectively, which are well smaller than the errors of the γ-ray energies.

The study of C-jets, made by two-storied emulsion chambers, revealed various features of multiple particle production in 10^{14} eV. Those are the violation of the Feynman scaling law, the increase of the average transverse momentum $< p_{T\gamma} >$, the correlation of $dN/d\eta$ *vs.* $< p_{T\gamma} >$, the jet structure of γ-ray emission, etc.[2]

All these features of multiple particle production in 10^{14} eV are confirmed by the experiments at CERN SPS $\bar{p}p$ collider, and Halzen *et al.* wrote, "Recent results from the UA1 and UA5 experiments at the CERN $\bar{p}p$ collider have shown that the emulsion chamber data up to $\sim$ 100 TeV (C-jets) are in good agreement with the accelerator data."[3]

We tried to describe the features of multiple particle production below and in 10^{14} eV by the production of small and large mass-constant fireball ($M_H = 2.5$ and $M_{SH} = 22.5$ GeV/c^2), because the distribution of the estimated fire-ball mass looks to consist of two groups.[2] However, the issue is not settled yet.

2. Violation of the Feynman scaling law in 10^{14}, 10^{16} and 10^{18} eV

Feynman speculated the scaling behavior of the inclusive cross section, which is expressed by $x(= 2p^*_{||}/\sqrt{s})$ and p_T, on the assumption that the cross section and the transverse momentum are

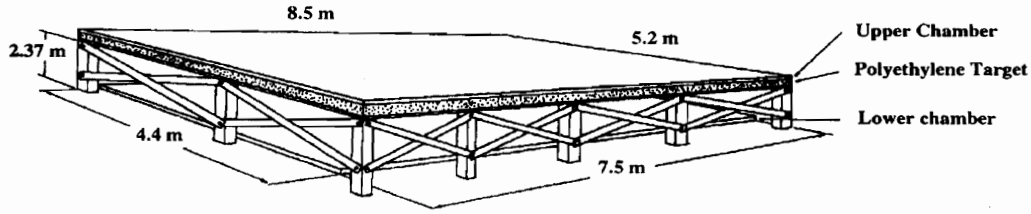

Figure 1. Two-storied emulsion chamber at Mt. Chacaltaya

independent of the incident energy.[1][4] It seemed to be valid up to the energy of $\sqrt{s} = 63$ GeV[5], and various empirical formulae are proposed for the scaling function, such as

$$\frac{dN}{dx} \equiv \frac{1}{\sigma_{inel}} \frac{d\sigma}{dx} = D\frac{(1-x)^d}{x} \qquad (1)$$

$$(x = \frac{E}{E_0},\ D = 1.67,\ d = 4.0)$$

which is for the produced *charged* particles.[7] However, in still higher energies, both the cross section and the transverse momentum are found to increase with the energy, and really the particle density dN/dx in the central region is enhanced to the scaling function. It is not settled yet whether the law is valid or not in the forward region, which is the most important in analyzing the cosmic-ray events.

We can discuss it in $10^{14} \sim 10^{15}$ eV, based on the data of direct observation of nuclear interactions. In $10^{16} \sim 10^{17}$ eV the discussion can be made indirectly by the cosmic-ray data. And highest energy air showers bear a clue to discuss it in $10^{18} \sim 10^{20}$ eV.

2.1. $10^{14} \sim 10^{15}$ eV

Fig. 2 shows the pseudo-rapidity density distribution of charged particles in the energy region of $10^{14} \sim 10^{15}$ eV from various sources. Experimental data comes from the accelerator experiments (UA5($\sqrt{s}$ = 546 GeV), UA7($\sqrt{s}$ = 630 GeV), Harr *et al.*($\sqrt{s}$ = 630 GeV))[8–10] and from the cosmic-ray experiment (C-jets).[11] The predictions by the various simulation codes are shown together.[12] One can see in Fig. 2;

(1) the experimental data of UA5, UA7 and C-jets are consistent with one another, and shows the suppression of the rapidity density in the forward region,[2] (Accordingly the resultant inelasticity decreases with the energy very slowly.)

(2) among the experimental data only those by Harr *et al.* show a higher density in the forward region,

(3) the densities in the forward region, predicted by the simulations, are enhanced to the scaling function, while they agree with the scaling function at $\sqrt{s} = 53$ GeV. (Accordingly the resultant inelasticity increases with the energy.)

By the above observation we are favorable to the suppression of the rapidity density in the forward region, which is supported by the data in still higher energy region, as mentioned below.

2.2. $10^{16} \sim 10^{17}$ eV

Direct observation of the nuclear interactions, or the observation of the nuclear interactions of the known interaction points, is not easy in this energy region, due to the scarce intensity of high energy cosmic-rays. The upper chamber of the

[1] The scaling behavior of the energy spectrum had been pointed out by emulsion chamber experiments.[6]

[2] UA7 Collaboration claimed the validity of the law *naively* in terms of $d\sigma/dy$, instead of $(1/\sigma_{inel})d\sigma/dy$, and criticized *incorrectly* the conclusion of the violation of the law, obtained by C-jet data.[9]

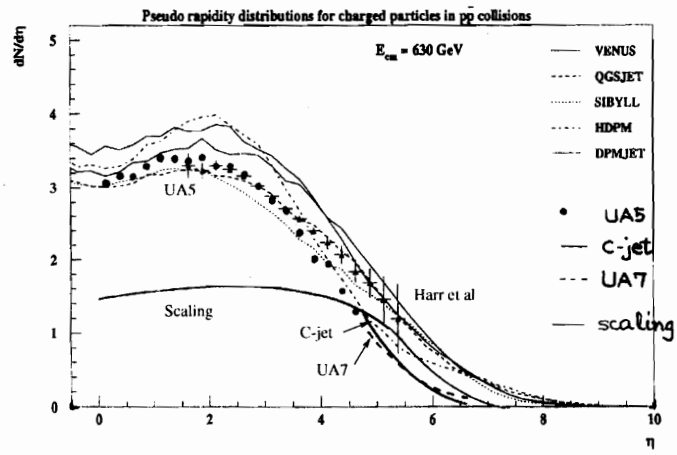

Figure 2. Pseudo-rapidity distributions of charged produced particles in multiple particle production at $s^{1/2} = 630$ GeV from various sources.

two-storied emulsion chamber and/or the flat-type emulsion chamber detect a bundle of particles which are produced through the nuclear interaction(s) in the atmosphere. The event is called "family" or "A-jet".

Fig. 3 shows the integral intensity of the families, where $\sum E_\gamma$ is the total energy observed in the family. The experimental data gives a smaller intensity of families than that by the simulation of cosmic-ray propagation in the atmosphere.[13] The simulation assumes UA5 algorithm for nuclear interactions in the atmosphere and the normal composition of the primary cosmic rays. The discrepancy of the family intensity between the experimental data and the simulation indicates more rapid energy subdivision either in the nuclear interaction or in the primary cosmic rays. Hence various hypotheses are proposed for the discrepancy, such as that the nuclear interaction changes its feature in high energy region (*i.e.* the violation of the scaling law, the existence of the exotic interactions, etc.) and that the composition of the primary cosmic rays becomes heavier (*i.e.* Fe-dominant composition). However, the issue is not settled yet, because the discussion in this way depends crucially on the assumed intensity of the primary cosmic rays which must be borrowed from another type of the experiment.

The family and the air shower are the different cut-edges of the same high energy cosmic-ray event, and the air shower size is a good measure of the primary energy which initiates the air shower. Hence it is possible to make the above discussion, without assuming the primary cosmic-ray intensity, by observing family and the accompanied air shower simultaneously. Fig. 4 shows the relation between the average of the total observed energy in the family and the size of the accompanied air showers, which is obtained by the experiment to operate the emulsion chamber and the air shower array simultaneously at Mt. Chacaltaya.[14] One can see in Fig. 4 that $< \sum E_\gamma >$ by the experimental data is smaller than that by the simulation. The same type of the experiment at Tien Shan (3,300 m, Kazakhstan) supports the conclusion, again.[15] And the discrepancy cannot be reconciled by the proposed heavy-dominant composition of the primary cosmic rays. It indicates that the nuclear interaction changes its feature more strongly than the UA5 code predicts

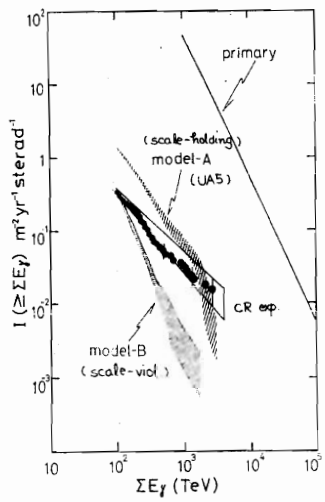

Figure 3. The integral intensity of families at Mt. Chacaltaya, where ΣE_γ is the energy sum of γ-rays in the family. The triangular area is the one with the error, obtained by the Chacaltaya emulsion chamber experiment, and the hatched area, indicated as "model-A", is by the simulation, mentioned in the text.

in higher energies.[3]

2.3. $10^{18} \sim 10^{20}$ eV

It is interesting to see how the scaling violation, observed in 10^{14} eV, affects the air shower development in the highest energy region, because there are projects to observe the air showers in this energy region and because it is under discussion why the GZK cut-off is not seen clearly in the primary cosmic-ray energy spectrum.

We constructed an empirical formula of pseudorapidity density of produced particles which reproduces the data by UA5, UA7 and C-jets, assuming that the Feynman scaling law breaks down gradually as the incident energy increases.[11] That is,

$$\frac{dN}{dx} = D\left(\frac{E_0}{A}\right)^{\alpha}\left[1-\left(\frac{E_0}{A}\right)^{\alpha'} x\right]^4 \frac{dx}{x} \qquad (2)$$

$$(A = 2.0 \text{ TeV},\ \alpha = 0.156,\ \alpha' = 0.161)$$

which is enhanced in the central region and suppressed in the forward region, in high energies. The formula converges to the scaling function of Eq.(1) at $E_0 = 2.0$ TeV, and predicts the total inelasticity of

$$K = 0.5\left(\frac{E_0}{A}\right)^{\alpha}\left(\frac{E_0}{A}\right)^{-\alpha'} = 0.5\left(\frac{E_0}{A}\right)^{-0.005} \qquad (3)$$

which decreases weakly with the incident energy.

Fig. 5 shows the development of air shower size for the incident proton of $E_0 = 10^{18}$ and 10^{20} eV, which are calculated analytically assuming Eq.(2) (the scale-breaking case) and the increasing cross section of

$$\lambda_{coll} = \lambda_0\left(\frac{E_0}{B}\right)^{-\beta} \qquad (4)$$

$$(\lambda_0 = 81.7 \text{ g/cm}^2,\ B = 1.0 \text{ TeV},\ \beta = 0.056)$$

The figure shows those of the scale-holding case (assuming Eq.(1)), too. The air shower size at the sea level does not differ so drastically between the two cases. However, if the violation of the law is stronger, as indicated by the data in $10^{16} \sim 10^{17}$ eV, the difference becomes larger between the two cases. Detailed discussion of the air shower development will be made elsewhere, assuming violation and no violation of the Feynman scaling law.

[3] The rapidity density distribution by UA5 simulation code shows a mild violation of the Feynman scaling law (suppression) in the forward region.

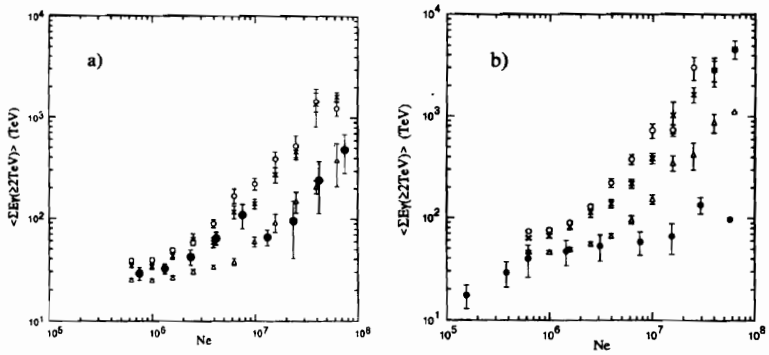

Figure 4. Shower size (N_e) dependence of the average family energy ($\sum E_\gamma$): (a) for the HADRON experiment at Tien-Shan, and (b) for the experiment at Mt. Chacaltaya. Symbols are; ○ for model-A (scale-holding) with 'normal' chemical composition, × for model-A with 'heavy-dominant' chemical composition, △ for model-B (scale-breaking) with 'normal' composition and • for experimental data.

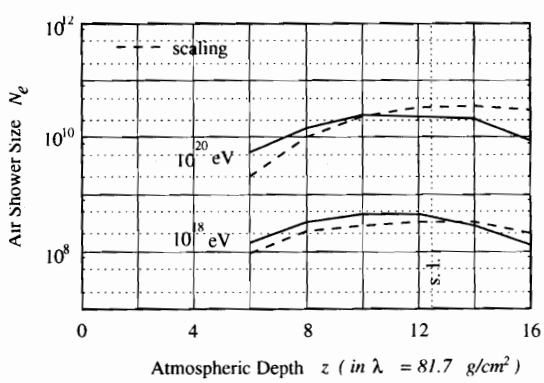

Figure 5. Development of the air shower size N_e along the atmospheric depth, for the cases of the incident proton of $E_0 = 10^{18}$ and 10^{20} eV. The solid (dashed) lines are on the assumptions of the scale-breaking (scale-holding) energy spectrum of the produced particles and of the increasing cross section. "s.l." stands for the sea level.

3. Centauro events

3.1. Centauro I and candidate events

If an air shower hits the two-storied emulsion chamber, we observe an event which consists of a number of showers, mainly due to γ-rays (and electrons), in the upper chamber and a few (or no) showers, due to C-jets and Pb-jets, in the lower chamber, because the hadron detection is limited. Most of the families bear such features.

However, in 1972 we encountered an event of contrasting feature in Chamber 15, called "Centauro I".[16] That is, the event consists of 7 showers (28.1 TeV in total) in the upper chamber, and of the ensemble (202.5 TeV in total) of 29 C-jets, 7 Pb-jets and 7 diffused showers in the lower chamber. The showers, found in the lower chamber, are surely of hadron origin, because no electron (photon) can arrive at the lower chamber without leaving any trace in the upper chamber. Furthermore, we could estimate the production height of the event as $H = 50 \pm 15$ m from the observed convergence of shower configurations at different depths in the lower chamber, which enables us to estimate the transverse momenta of produced particles.

We reach the conclusion that Centauro I is the multiple production of 74 hadrons without emission of γ-rays (electrons). These hadrons have transverse momenta of $< p_T >= 1.8$ GeV/c. The exotic points of Centauro I are listed in Table 1 with some remarks. We tried to describe Centauro I phenomenologically by the multiple $N\bar{N}$ production (N : nucleon), taking into account the facts that $< p_T >$ is larger than that of pions and that γ-rays are not produced.

Several candidates of the Centauro event are accumulated by the series of exposure of two-storied emulsion chamber at Mt. Chacaltaya, although their hadron-rich nature is diluted by some γ-rays, probably owing to their production height at higher altitude. Fig. 6 shows these events together with all the observed families with $\sum E_{ob} \geq 100$ TeV.

The abscissa expresses the ratio of the observed hadron energy to the observed total energy, defined by

$$Q_h = \frac{\sum E_h^{(\gamma)}}{\sum E_h^{(\gamma)} + \sum E_\gamma}$$

($E_h^{(\gamma)}$: the energy of the shower by hadron)

3.2. The Centauro event, found recently.

One more distinct example of the Centauro event was found in Chamber 22 during our routine process of measurement.[17] We found that a cluster of showers in the lower chamber has no corresponding part in the upper chamber. It is of no doubt by the direction of the showers in the lower chamber that the event passes the upper chamber. Careful search of the showers in the upper chamber was repeated assuming various errors in shower direction measurement, but was not successful.

The reason why this event was left for the routine process of measurement, in spite of our Centauro scanning which is always made immediately after the photo-processing of the sensitive materials, is;

(1) There are two families in the upper chamber, which appear to correspond to the cluster of showers in the lower chamber. However, this correspondence was found wrong by the routine process of measurement.

(2) The Centauro search was made mainly in the energy region of $\sum E_{ob} \geq 100$ TeV.

We are sure that such mis-correspondence is quite rare.

The characteristics of this new event is listed in Table 2 in contrast to Centauro I.

The fact that no shower is observed in the upper chamber indicates that the event is produced near above the chamber, too. Furthermore, one should notice that the new event has a low energy.

3.3. Probabilities of Centauro events.

We discuss two kinds of probability for Centauro events.(Table 3) One is the probability p_1 that the Centauro event is observed among the families experimentally, and the other is the one p_2 that the Centauro event is expected by the simulation where the normal multiple particle production is assumed.

(1) The total exposure of two-storied emulsion chambers (from Chamber 15 to Chamber 22)

Table 1 Characteristics of Centauro I

Primary Energy	1,650 TeV	assuming $K = 1.0$ and $< k_\gamma >= 1/6$
Production Height	50 ± 10 (m) above the chamber	strong penetration into atmosphere (500 g/cm^2)
Multiplicity of secondaries	74	large
Multiplicity of π^0's	0	???
$< p_T >$ of secondaries	1.8 GeV/c	$c.f.$ $< p_{T\pi^0} >= 0.4$ GeV/c

Table 2 Centauro I and the new event

	ΣE_{ob} (TeV)	No. Obs. Showers Upper Ch.	Lower Ch.	Estimated Primary Energy (eV)
Centauro I	221.6	7	43	1.6×10^{15}
The new event	51.2	0	13	3.1×10^{14}

Table 3 Probability of Centauro events.

Event	$\sum E_{ob}$ (TeV)	$I(> \sum E_{ob})$ (m·yr·sr)	Prob. p_1 Expected. No. of Families	p_1	Prob. p_2
Centauro I	221.6	0.33	80	1.2×10^{-2}	1.0×10^{-5}
The new event	51.2	2.08	772	1.3×10^{-3}	2.0×10^{-6}

Table 4 Origin of Centauro event.

	Interaction Origin	Primary Origin
Energy Sp.	$\propto dE/E$	$\propto \delta(E-a)dE$
$< p_T >$	large	~ 0
Threshold Energy	Yes	No
Surviving Particle	Yes	No
Accelerator Exp.	Yes	No
Deep Penetration	No	Possible

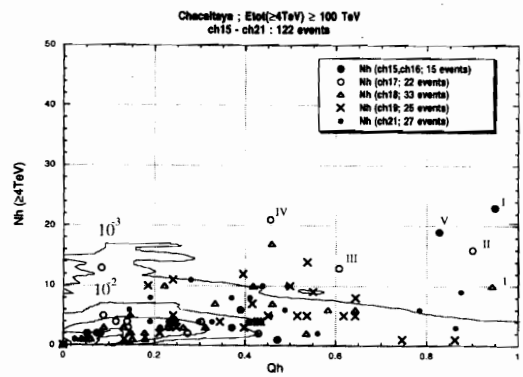

Figure 6. N_h(the number of hadrons) $- Q_h$ diagram of all the families ($\sum E_\gamma \geq 100$ TeV, $E_{th} \geq 4$ TeV), observed by two-storied emulsion chambers (Ch. 15 $\sim$ Ch. 21) at Mt. Chacaltaya. Centauro candidates are shown by the marks (I $\sim$ V and 1). The contours expresses the normalized density of the simulated events.

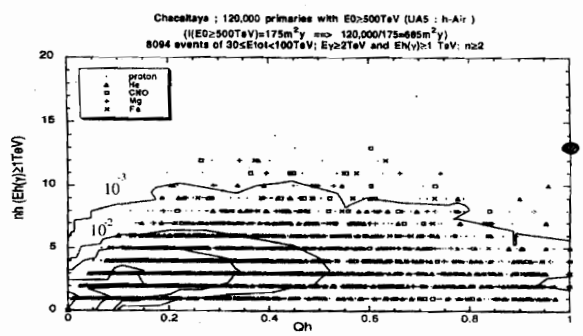

Figure 7. $N_h - Q_h$ diagram for the new event. One should notice that the difference of the detection threshold energy between in this event and in those of Fig. 6. The event is shown by the largefull circle and the simulated events by small marks. The contours express the normalized density of the simulated events.

amounts $ST = 3.49 \times 10^2$ (m^2·yr). The intensity of families with the total observed energy $\sum E_{ob}$ (with $E_{ob} > 4$ TeV) is given by

$$I(> \Sigma E_{ob}) = 0.90\left(\frac{\sum E_{ob}}{100\ \mathrm{TeV}}\right)^{-1.25\pm0.10} \quad (5)$$

$$(/\mathrm{m}^2\cdot\mathrm{yr}\cdot\mathrm{sr}\ )$$

in $\sum E_{ob} = 100 \sim 3000$ TeV.[13] Hence we can calculate the probability of the Centauro event among the observed families (assuming that the sensitive solid angle of the emulsion chamber is $\Omega = 0.7$), which are shown in Table 3.

(2) Fig. 6 presents the contours of the normalized density of the simulated events (1622 events with $10^2 \leq \sum E_{ob}$ (TeV) $\leq 10^4$). The conditions for the family is $E_{th} = 4$ TeV and $n_{shower} \geq 3$.

Noticing that the contour is almost in parallel with the abscissa in $Q_h = 0.8 \sim 1.0$, we estimate the probability of Centauro I. That is, the probability of one event with $N_h = 16$ and $Q_h = 0.8 \sim 1.0$ is 1.0×10^{-5}.

Fig. 7 is for the new event. The conditions for the family is $E_\gamma > 2$ TeV, $E_h^{(\gamma)} > 1$ TeV, and $n_{shower} \geq 2$, and number of simulated events is 8094 with $30 \leq \sum E_{ob}$ (TeV) ≤ 100. The probability of one event with $N_h = 13$ and $Q_h = 0.9 \sim 1.0$ is 2.0×10^{-6}.

The difference between p_1 and p_2 shows that the Centauro events cannot be produced by the fluctuation of the multiple particle production and/or of the collision mean free path.

3.4. Origin of Centauro; exotic interaction or exotic primary ?

Since the discovery of Centauro I in 1972, various hypotheses for the Centauro event are proposed by many authors. Those are classified into two categories of interaction origin and primary origin. That is, the Centauro event is produced through some exotic mechanism in the interaction of known hadron(s) with atmospheric nucleus, such as DCC by Bjorken, strangelet by Angelis *et al.*, etc.[18] Or it is produced by some exotic particle among the primary cosmic rays, such as quark glob by Bjorken, strange quark matter by Witten, etc.[19] However, it is our regret to say that none of these interesting hypotheses can describe the Centauro events fully and convincingly.

We try to discuss to which origin, interaction or primary, the data on our hands are favorable. We assume that, if the Centauro event is of interaction (primary) origin, the features of the produced hadrons is similar to those by multiple particle production (fragmentation of nucleus). Then,

(1) The energy spectrum of produced hadrons is $\propto dx/x$ ($\propto \delta(x-a)dx$).

The energy spectrum of observed showers, induced by the produced hadrons, does not differ so distinctly between the two cases.

(2) The transverse momenta of produced particles are relatively large (small).

The estimated value of $< p_T >$ in Centauro I is larger.

(3) There is a (no) threshold energy for the production of the Centauro events.

The new event has relatively low energy.

(4) There does (not) exist a surviving particle, though not necessarily.

Centauro V contains one shower of very high energy compared with other showers. It might be identified as the surviving hadron.

(5) The Centauro events are (not) observed by the accelerator experiments.

Results of Centauro search by UA1 and UA5 Collaborations are negative.

(6) An incident hadron of known type cannot, but exotic primary particle might, penetrate deep in the atmosphere without interaction.

The discussion is summarized in Table 4, where the underline means "indicated by the experimental data". Taking into account that the weight of respective item in Table 4 is not equal, one can see that there is no decisive data yet to choose one of them.

Acknowledgment

The author thanks Prof. Oscar Saavedra (the chairman) and other members of the Local Organizing Committee of the Symposium for offering him an opportunity to give a present talk and for holding a successful and enjoyable symposium. He also is grateful to the members of Chacaltaya Emulsion Chamber Collaboration for many en-

lightened discussions.

REFERENCES

1 C.M.G. Lattes *et al.*, Prog. Theor. Phys. Suppl. No.47 (1971) 1.
2 J.A. Chinellato *et al.*, Prog. Theor. Phys. Suppl. No.76 (1983) 1.
3 F. Halzen *et al.*, Nucl. Phys. **B190** (1987) 213.
4 R. Feynman *et al.*, Phys. Rev. Lett. **23** (1969) 1415.
5 F.E. Taylor *et al.*, Phys. Rev. **D14** (1976) 1217.
6 M. Akashi *et al.*, Prog. Theor. Phys. Suppl. No.32 (1965) 1.
7 T.K. Gaisser *et al.*, Rev. Mod. Phys. **50** (1978) 859.
8 G.L. Alner *et al.*, Z. Phys. **C33** (1986) 1; Nucl. Phys. **B291** (1987) 445; Phys. Rep. Nos. 5 and 6 (1987) 247.
9 E. Pare *et al.*, Phys. Lett. **B242** (1990) 531. M. Haguenauer *et al.* Proc 20 Internat. Cosmic Ray Conf. Vol.5 (1987) 23.
10 R. Harr *et al.*, Phys. Lett. **B401** (1997) 176.
11 A. Ohsawa, Prog. Theor. Phys. **92** (1994) 1005.
12 J. Knapp *et al.*, Preprint of Forschunkszentrum Karlsruhe FZKA 5828 (1996).
13 L.T. Baradzei *et al.*, Nucl. Phys. **B370** (1992) 365.
14 N. Kawsumi *et al.*, Phys. Rev. **D53** (1996) 3534.
15 M. Tamada, J. Phys. G **20** (1994) 487.
16 C.M.G. Lattes *et al.*, Phys. Rep. **65** (1980) 65.
17 S.L.C. Barroso *et al.*, Proc. 25 Internat. Cosmic Ray Conf. Vol. 6 (1997) 53.
18 J.D. Bjorken, Int. J. Mod. Phys. **A7** (1992) 4189.
A. Angelis *et al.*, a talk in this symposium.
19 J.D. Bjorken *et al.* AIP Conf. Proc. No.49 (1978) 509; Phys. Rev. **D20** (1979) 2353.
E. Witten, Phys. Rev. **D30** (1984) 272.

NAME | ID No | M.S.